

L. GUERRA-ROSA* and L. O. FARIA*

The causes of failure in bearing screws, which led to the collapse of the jib of a travelling crane, are analysed. The travelling crane had a capacity of 50 metric ton x 30 m / 20 metric ton x 48 m and it worked in a shipyard for several years. Fatigue and stress corrosion cracking was detected. A stress analysis is presented taking into account the stress concentrations at the screws. The accident is explained applying fracture mechanics concepts and considering the material parameters, namely ΔK_{th} and K_c . The poor design of the screws, the insufficient locking device, their mounting without control of the tightening torque, a non-existing maintenance, and corrosion due to the environment, are the main causes of this failure.

DESCRIPTION OF THE EQUIPMENT

A travelling crane working for several years in a shipyard collapsed due to the fracture of the screws of its jib pivot. The travelling crane had a capacity of 50t x 30m/20t x 48m and at the moment of the accident was handling a lower load at 30m. The pivot of the crane lib was composed of two bearings split in two halves kept by six screws each. A sketch of the travelling crane is presented in fig. 1. Figure 2 shows the bearings and table I indicates the geometry of the screws.

TABLE I - Screws geometry

Hexagonal head.

Type of thread : Whitworth, $\theta = 55^\circ$

Thread dimensions of the fractured screws:

External diameter $\phi_{ext} = 41.21 \text{ mm}$

Internal diameter $\phi_{int} = 34.77 \text{ mm}$

Depth of thread $H = 3.22 \text{ mm}$

Pitch $p = 5.08 \text{ mm}$ (5 threads per inch)

Cross section area at external diameter $A_e = 1334.07 \text{ mm}^2$

Cross section area at internal diameter $A_i = 949.56 \text{ mm}^2$

Rounded root radius $\rho = 0.15 \text{ mm}$ (mean value)

Plain part of screw : same diameter of external diameter of thread.

* CEMUL - Centre of Mechanics and Materials, Technical University of Lisbon, 1096 LISBOA CODEX, PORTUGAL.

SCREWS MATERIAL PROPERTIES

The screws material has been tested in order to determine its metallurgical and mechanical properties. The results are as follows.

Chemical Composition of Steel

C	Mn	Si	Cr	Ni	Cu	Mo	Zn	S	P
0.32	0.60	0.20	0.18	0.15	0.17	0.037	0.025	0.042	0.032

Microstructure

Metallographic observations revealed a normalized ferritic-pearlitic microstructure. Grain size was number: 4-5 (ASTM) with a median grain diameter $\bar{d} = 78 \mu\text{m}$ (according to the Heyn method).

Tensile Strength

Hardness : $H_V = 2000 \text{ N mm}^{-2}$ (mean value).

Tensile tests :

Screw No.	Specimen No.	Spec. diameter (mm)	σ_{UTS} (MPa)	σ_Y (MPa)	ϵ_{max}^* (%)
1	4	4.5	634.7	—	17
1	5	4.5	644.6	—	16
2	13	4.5	630.1	—	15
2	14	4.5	638.3	—	15
2	—	5.5	643.5	383.6	23

According to the chemical analysis and the tensile tests results, the screws steel may be considered as a St 60 (DIN 17100).

Fracture Toughness

Fracture toughness tests were conducted according to BS 5762 [1]. Three-point bend test pieces with different thicknesses ($B = 9.9, 15.0, 19.9$ and 28.8 mm) were used in order to study the influence of r_p/B on the measured K_{IC} - values as suggested in [2]. In all test pieces the crack plane was perpendicular to the screw axis.

The load vs. clip gauge displacement graphs were of type (iii) [1] for all test pieces. This type of graph is schematically represented in fig.3. Table II shows the fracture toughness results. The K_{IC} - values were not calculated from P_u but from P_5 using the formula:

$$K_{IC} = \frac{Y P_5}{B \sqrt{W}} \quad (1)$$

where P_5 is the load corresponding to the intersection point of the secant line OP_5 drawn through the origin of each test record with slope $(P/v)_5 = 0.95 (P/v)_0$, where $(P/v)_0$ is the slope of the tangent OA to the initial linear part of the record. In the authors' opinion this is a more

* Gauge length $l_0 = 12.5 \text{ mm}$ except for 5.5 mm - diameter specimen ($l_0 = 25 \text{ mm}$).

reliable method to estimate K_{IC} values, instead of calculating K_{IC} from P_u , because the usual Y values are calculated for linear elastic behaviour, not taking into account the yielding effect.

TABLE II - Fracture toughness results

Screw No.	Specimen No.	Thickness, B (mm)	δ_u^* (mm)	$K_{IC}^{-3/2}$ ($\text{MN m}^{-3/2}$)	r_p/B	P_u/P_5
1	A1	9.9	0.22	71.30	0.656	1.51
1	A2	9.9	0.17	70.32	0.638	1.50
2	B1	15.0	0.20	65.24	0.363	1.45
3	C2	19.9	0.11	52.40	0.176	1.28
5	D1**	28.8	0.08	41.17	0.075	1.21

Crack-tip plastic zone sizes, r_p , were estimated for the plane stress ($P\sigma$) condition existing at the specimen surface according to ref. [3]:

$$r_p = 0.188 \left(\frac{K_{IC}}{\sigma_Y} \right)^2 \quad (2)$$

Figure 4 shows the effect of r_p/B on fracture toughness and indicates that plane strain ($P\epsilon$) conditions prevail in the 28.8 mm thick specimen.

Fatigue Crack Propagation

During the fatigue precracking of the three-point bend test pieces, some da/dN vs. ΔK data was obtained for each specimen. Fatigue crack propagation was carried out in a load controlled closed loop hydraulic fatigue machine, applying a sinusoidal load wave with 25 Hz cyclic frequency, at a stress ratio $R = 0.1$. The secant method was used and the results are presented in Table III and fig.5.

STRESS ANALYSIS

Considering the friction between threads and between screw head and bearing cap surfaces, and applying the Von Mises theory, the equivalent normal stress at each screw would be:

$$\sigma_{eq} = 1.6 \frac{F}{A} \quad (3)$$

F being the applied force to the screw.

The stress concentration factors are approximately as follows:

- between screw head and plain part of the screw : $k_1 = 2.14$
- between plain part and threaded part : $k_2 = 1.42$
- between screw thread and threaded bearing : $k_3 = 3.56$

The maximum tensile load at each screw, corresponding to the most unfavourable position of the crane jib is $F = 110\,000 \text{ N}$.

* Calculated according to BS 5762 : 1979.

** For specimen D1, $B > 2.5 \left(\frac{K_{IC}}{\sigma_Y} \right)^2$. However, as the ratio P_u/P_5 exceeded 1.1, K_{IC} can not be taken as a valid K_{IC} - value.

TABLE III - Fatigue Crack Propagation Results

Specimen No.	ΔK ($MN m^{-3/2}$)	da/dN ($mm/cycle$)
A1	15.5	1.2×10^{-5}
A1	23.3	5.0×10^{-5}
A2	11.8	5.3×10^{-6}
A2	20.9	2.3×10^{-5}
B1	24.7	5.6×10^{-5}
B1	26.4	6.5×10^{-5}
C2	29.9	8.1×10^{-5}
C2	31.4	9.8×10^{-5}
D1	9.3	3.0×10^{-6}
D1	12.1	7.2×10^{-6}

Neglecting the initial stress due to subsequent reduction of the friction moment after tightening, but considering the maximum stress concentration factor, the maximum normal stress at each screw is:

$$\sigma_{max} = k_3 \frac{F}{A_i} = 412 \text{ MPa} \quad (4)$$

The occasional forces acting perpendicularly to the screws axis, due to the clearance between the journal and the bearing were not taken into consideration, as the existing clearances between the screws and the corresponding holes in the bearings do not allow any shear stress.

FRACTOGRAPHIC OBSERVATIONS

Table IV summarizes the observations made by visual inspection and also using Scanning Electron Microscopy (SEM) in the screws of the two bearings.

FRACTURE MECHANICS ANALYSIS

Nucleation of cracks at the thread root

Taking into consideration the dynamic loading of the crane, the stress-intensity range at the jib bearing screws should be, since $K_{min} \approx 0$,

$$\Delta K = K_{max} - K_{min} \approx K_{max} \quad (5)$$

There are different ways to estimate the stress-intensity factor at the thread root:

i) As shown in [4] the following equation can be used:

$$K = 1.12 \sigma_{max} \sqrt{\pi d} \quad (6)$$

where σ_{max} is the concentrated stress at the thread root given by equation (4) and $d = \text{grain size} = 78 \mu m$. $\Delta K \approx K_{max}$ calculated from

TABLE IV - Fractographic inspection

Screw No.	Aspect of fracture surface	Position of fracture surface	Remarks
1	3 mm deep fatigue crack; the rest of the surface presented the characteristic aspect of a stress corrosion fracture.	At the plane of separation of the bearing halves.	See fig.6.
2	About 15 mm deep fatigue crack; the rest of the surface exhibited an almost brittle fracture.	Inside the threaded part of the bearing half.	Rest of the loosened screw. Screw part attached to the head was not found. Fracture probably occurred prior to the accident.
3	14 mm deep fatigue crack; the rest of the surface exhibited an almost brittle fracture.	Inside the threaded part of the bearing half.	See fig.7.
	13 mm deep fatigue crack; followed by + 14 mm (depth) brittle fracture.	Near the plane of separation of the bearing halves.	Complete fracture has not occurred in this crack.
4, 5, 6	Brittle fracture	At the plane of separation of the bearing halves.	Small fatigue cracks (about 1 mm deep) nucleated from the thread root could be detected on the fracture surface.
Screws of the other bearing	Brittle fracture		

equation (6) gives:

$$\Delta K \approx K_{max} = 1.12 \times 412 \sqrt{\pi \times 78 \times 10^{-6}} = 7.22 \text{ MNm}^{-3/2} \quad (6.a)$$

However, if the thread is considered as a notch for the plain part of the screw, the following formula should be used:

$$K = K_F \sigma_{nom} \sqrt{\pi d} \quad (7)$$

where K_F is the stress concentration factor in fatigue loading which takes into account the stress gradient ahead of the notch (considering

the occurrence of un-constrained plasticity during the nucleation stage as discussed in reference [5]) and given by $K_F = (1 + 6.79 \sqrt{H/\rho})^{1/2}$

(with $H =$ thread depth $= 3.22$ mm and $\rho =$ contour radius at thread root $= 0.15$ mm). σ_{nom} is the nominal stress in the plain part of the screw (A_e as defined in Table I):

$$\sigma_{nom} = \frac{F}{A_e} = 82.45 \text{ MPa} \quad (7.a)$$

In this case ΔK at the thread root, calculated from equation (7), is:

$$\Delta K \approx K_{max} = 7.35 \text{ MNm}^{-3/2} \quad (7.b)$$

ii) Another and perhaps more realistic way to estimate K at the thread root is to consider that short cracks (with a depth approximately equal to the grain size) are always present at the thread root as a consequence of the manufacturing process. In this case the thread would behave as a sharp crack (with constrained plasticity at the crack tip) and since H , the thread depth, is incomparably larger than the short crack depth the value of K is given by:

$$K = Y \sigma_{nom} \sqrt{\pi H} \quad (8)$$

where Y is still nearly 1.12 according to reference [6].

Using equation (8) which accounts for the above-mentioned pre-existing (short) cracks, ΔK at the thread root becomes

$$\Delta K \approx K_{max} = 9.29 \text{ MNm}^{-3/2} \quad (8.a)$$

In order to justify the occurrence of fatigue crack growth from the thread root the condition $\Delta K \approx K_{max} > \Delta K_{th}$ must be fulfilled. Fatigue tests carried out on similar ferritic-pearlitic steels [4, 7-9] give values for ΔK_{th} between 6 and 7 $\text{MNm}^{-3/2}$ for $R \approx 0$ (see also fig. 5) and still lower for higher R -values. Since all equations (6), (7) and (8) give ΔK -values greater than ΔK_{th} (without being necessary to discuss which equation is more realistic) nucleation and growth of a fatigue crack at the thread root can be easily predicted as, in fact, it occurred.

Long cracks emanating from the thread root

Long cracks emanating from the thread root due to fatigue or stress corrosion had a semi-elliptical shape (perpendicularly to the axis of the screw) as those studied by Athanassiadis et al. [10]. Usually the length of the crack front $2b$ and the crack depth a are related, so that the ratio a/b evolves toward the value 0.75 which corresponds to the uniform K distribution along the crack front as verified in [10]. Fracture occurs when $K = K_c$ and the K -values can be computed from:

$$K = Y \sigma_{nom} \sqrt{\pi a} \quad (9)$$

where a is the "total" crack depth (thread depth H plus crack depth due to fatigue or stress corrosion cracking).

SOME CONCLUSIONS

i) A LEFM analysis is enough to explain not only the occurrence of fatigue cracks emanating from the thread root but also the final collapse:

Screw no. 2 probably fractured first due to fatigue cracking. According to the fractographic inspection screw no. 1 fractured by a stress corrosion cracking process that occurred after the growth of a 3 mm deep fatigue crack.

Subsequently followed the fracture of screw no. 3 since the K_c -value was attained at the 14 mm deep fatigue crack, i.e., this fatigue-nucleated crack has grown under the spectrum cyclic loading till it reached the critical depth $a_c = 3.2 + 14 = 17.2$ mm (see Table IV). Using equation (9) with $K_c = 40 \text{ MNm}^{-3/2}$ (see fig. 4), $a = 17.2$ mm and $Y \approx 0.8$ (according to [6]) the required stress for fracture is $\sigma_{nom} = 215 \text{ MPa}$ which is easily attained in screw no. 3 considering that the load in this bearing is only taken by four screws (no. 3, 4, 5 and 6).

As soon as screw no. 3 severed by fracture, all remaining screws in both bearings collapsed right away as they were submitted to higher tensile stress and other secondary stresses (bending, shear).

ii) This accident is due in the authors' opinion to the fact that some fundamental rules in design and maintenance were not followed:

- a) The plain part of screws should have a diameter equal to the thread internal diameter in order to reduce the stress concentration; or, at least, the length of the threaded part should be increased.
- b) Fractured screws had not a sufficiently rounded thread-root contour. The root radius ρ should be larger (at least $\rho = 0.8$ mm) to prevent crack growth at this critical area.
- c) A magnetic particle inspection performed on all screws also detected cracks in the region between the screw head and the plain part of the screw. So, the fillet radius (transition to the screw head) should be increased to reduce the stress concentration and to avoid crack nucleation.
- d) The tightening should be controlled. It would be also recommended to replace the screws by bolts as the tightening torque is more effective.
- e) For 42 mm - diameter screws the use of spring washers does not prevent they get loose. A lock nut or other effective locking device should be preferable.
- f) A periodical inspection of such type of cranes should be compulsory in order to assure, in this particular case, that the screws were not getting loose and that a grease protection against the corrosive environment was kept in good condition.

SYMBOLS USED

- σ_y - 0.2% proof stress
 ϵ_{max} - engineering strain at σ_{UTS}
 Y - stress intensity coefficient
 r_p - plastic zone size ahead of the crack tip
 W - test piece width
 v - clip gauge displacement
 δ_u - crack opening displacement (COD) at unstable fracture
 R - minimum load/maximum load
 ΔK_{th} - threshold stress intensity factor below which fatigue crack growth will not occur.

REFERENCES

1. BS 5762 : 1979 "Methods for Crack Opening Displacement (COD) Testing", British Standards Institution.
2. HERTZBERG, R.W., "Deformation and Fracture Mechanics of Engineering Materials", J. Wiley & Sons, (1976) pp. 279-282.
3. GUERRA-ROSA, L., BRANCO, C.M. and RADON, J.C., "Monotonic and Cyclic Crack Tip Plasticity", *Int. J. Fatigue*, Vol. 6, No. 1 (1984) pp. 17-24.
4. GUERRA-ROSA, L. and BRANCO, C.M., "Influence of Plastic Zone Size on Fatigue Threshold in Steels", *Proceedings Inter. Conf. on Fracture Prevention in Energy and Transport Systems*, Rio de Janeiro, Brazil, E.M.A.S., November 1983, pp. 24-33.
5. SMITH, R.A., "Fatigue Threshold - A Design Engineer's Guide through the Jungle", *Fatigue Thresholds*, Proc. of an Intern. Conf. held in Stockholm, E.M.A.S., Vol. 1, (1981) pp. 33-44.
6. ROOKE, D.P. and CARTWRIGHT, D.J., *Compendium of Stress Intensity Factors*, H.M.S.O., London, (1976) pp. 297-299.
7. GUERRA-ROSA, L., BRANCO, C.M. and RADON, J.C., "Effects of Plasticity and Strain Rate on Fatigue Crack Growth", *Proceedings of the 4th European Conference on Fracture* held in Leoben, Austria, E.M.A.S., Vol. 2, September 1982, pp. 499-456.
8. Yu CHONGHUA and Yan MINGGAO, "A Calculation of the Threshold Stress Intensity Range for Fatigue Crack Propagation in Metals", *Fat. Engng. Mat. Struct.*, Vol. 3 (1980) pp. 189-192.
9. LINDLEY, T.C. and RICHARDS, C.E., "Fatigue Crack Growth at Low Stresses in Steels", Central Electricity Research Laboratories, Leatherhead Report No. RD/L/N 135/78 (1978).
10. ATHANASSIADIS, A., BOISSENOT, J.M., BREVET, P., FRANÇOIS, D. and RAHARINAIVO, A., "Linear Elastic Fracture Mechanics Computations of Cracked Cylindrical Tensioned Bodies", *Int. J. Fracture*, 17 (1981) pp. 553-566.

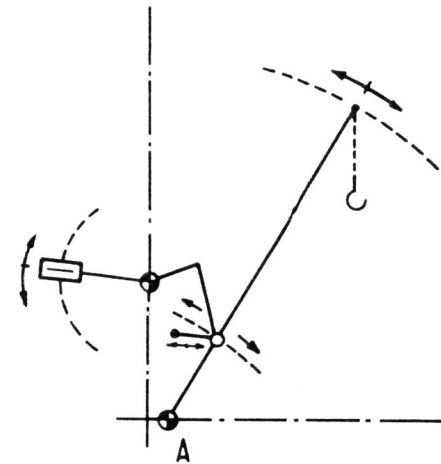


FIG. 1 - Sketch of the travelling crane showing the position of the bearing A in which screws fracture occurred.

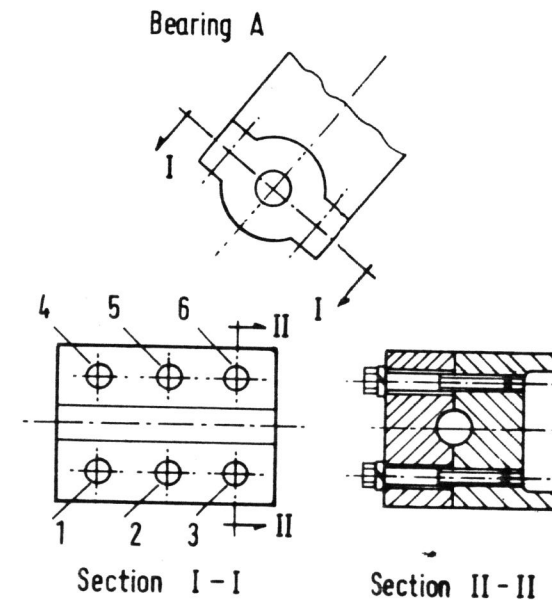


FIG. 2 - Schematic drawing of bearing A.

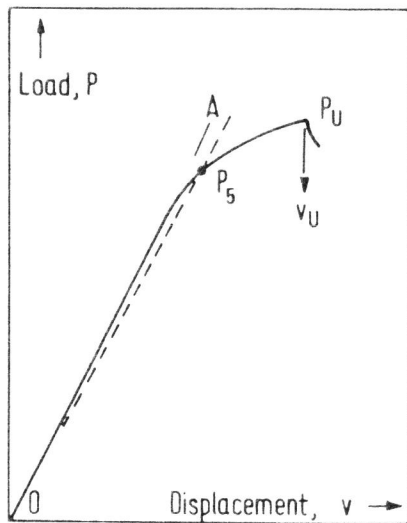


FIG. 3 - Type of load-displacement records obtained during COD testing.

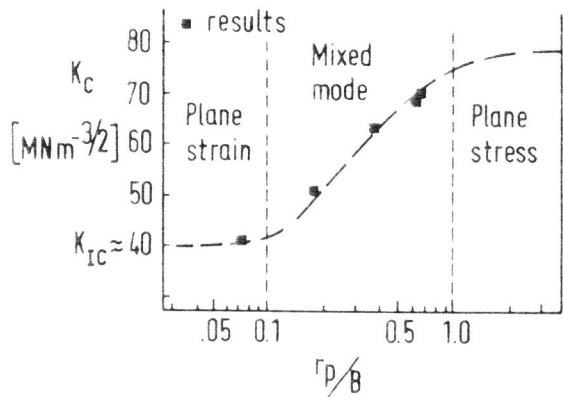


FIG. 4 - Effect of relative plastic zone size to specimen thickness on fracture toughness.

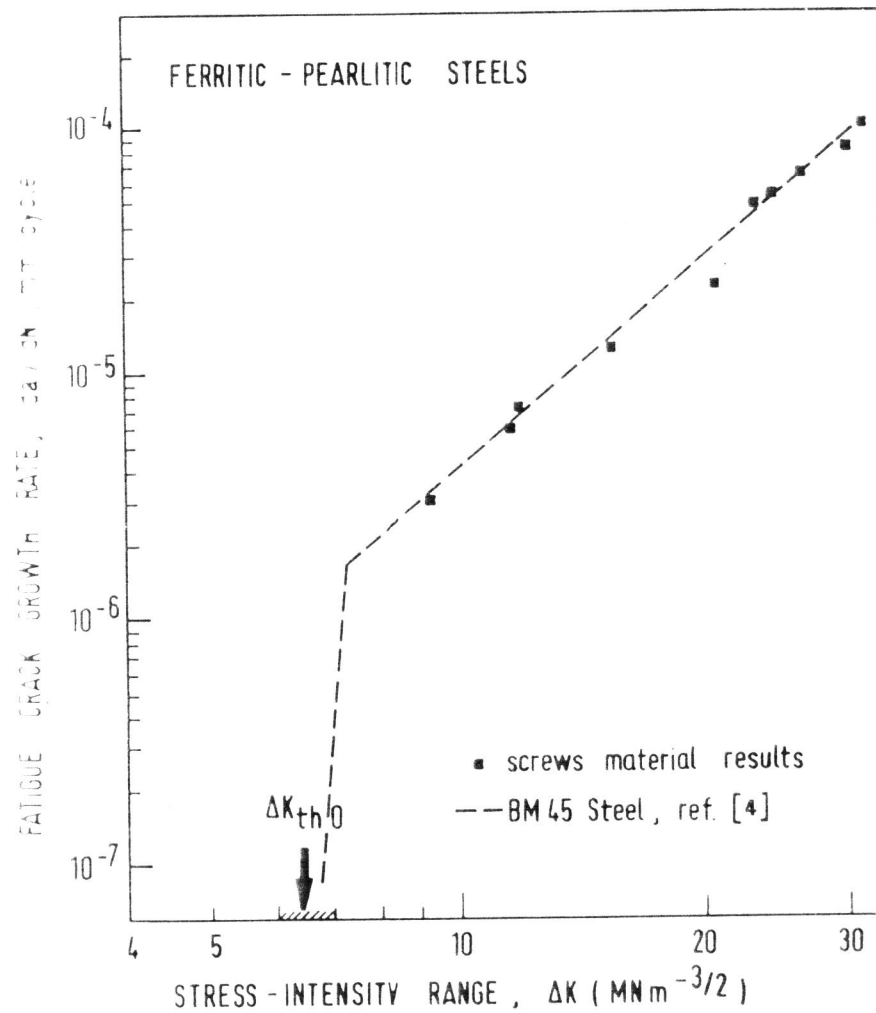


FIG. 5 - Fatigue crack propagation results for $R = 0.1$. Threshold gamut of similar steels for $R = 0$ is also indicated [8,9].

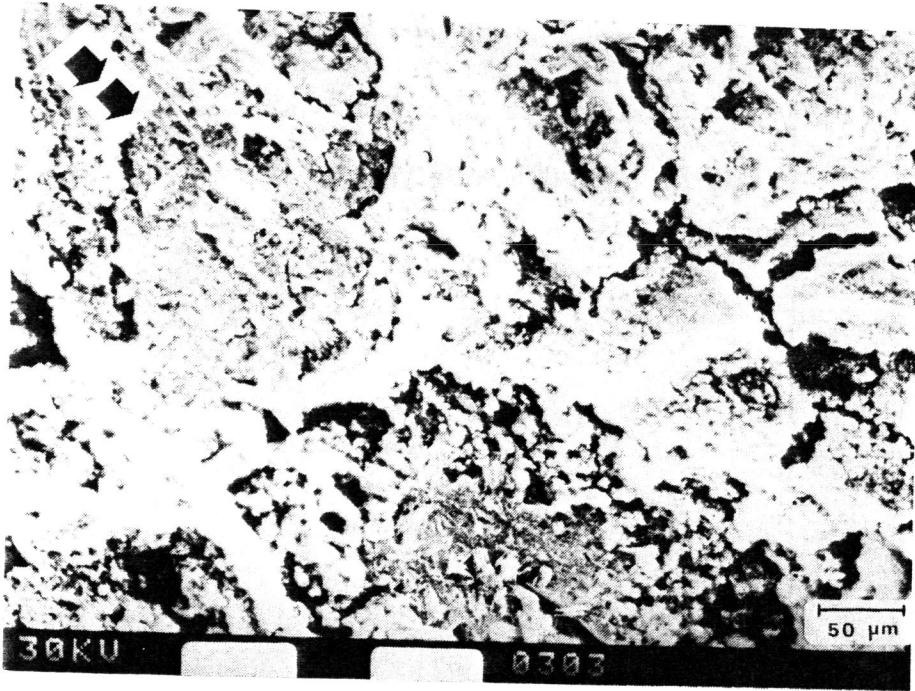


FIG. 6 - Fracture surface detail of screw No. 1 revealing stress corrosion cracking. (Arrows indicate direction of crack growth.) SEM, 300X.

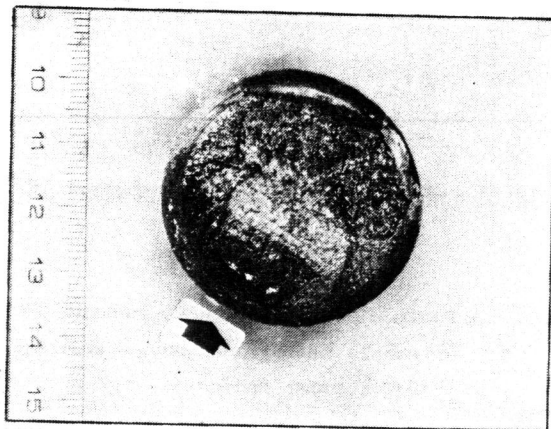


FIG. 7 - Fracture surface of screw No. 3.
(Arrow indicates direction of crack growth).